Dalton Transactions

ROYAL SOCIETY OF CHEMISTRY

PAPER

View Article Online
View Journal | View Issue

Cite this: *Dalton Trans.*, 2023, **52**, 14123

Mechanistic insight into cobalt-mediated [2 + 2 + 2]-cycloaddition reactions with γ-alkylidenebutenolide and γ-alkylidenebuterolactam as 2π partners†

Léo Chaussy, ‡ Marion Delorme,‡ Alexander Punter, Yannick Carissan, Jean-Luc Parrain, Muriel Amatore,* Paola Nava * and Laurent Commeiras *

Received 19th July 2023,
Accepted 20th September 2023

DOI: 10.1039/d3dt02291a

rsc.li/dalton

The molecular complexity of recently reported cobalt(III) polycyclic complexes, resulting from an intramolecular formal (2 + 2 + 3) cycloaddition reaction on an enediyne containing a lactone moiety, has prompted us to computationally review the mechanisms of cobalt cycloaddition reactions with γ-alkylidenebutenolide or γ-alkylidenebuterolactam as 2π partners. Computed mechanisms are compared, leading to either cobalt(III)- or cobalt(I)-spiro complexes depending of both the nature of the reaction (intra- *vs.* intermolecular pathway) and the nature of the 2π partner (γ-alkylidenebutenolide *vs.* γ-alkylidenebuterolactam). These proposed mechanisms are supported by experiments, allowing us to report the synthesis and characterization of the predicted compounds.

Introduction

Among synthetic strategies, metal-catalysed cyclotrimerisations of alkynes represent elegant approaches to functionalised aromatic and heteroaromatic polycyclic systems.[1] [2 + 2 + 2] cycloaddition reactions are also convenient solutions for the synthesis of cyclohexadiene cores when two alkynes and one alkene are engaged as 2π partners in the process.[2] Among active species for metal-mediated or metal-catalysed [2 + 2 + 2] cycloaddition reactions, $CpCoL_2$ (L = CO, PR_3, alkenes) complexes have proven their efficiency both for the synthesis of arenes and cyclohexadienes. In this context, the general mechanism of the cobalt-catalysed process involving two alkynes and one alkene has been proposed based on both experimental and computational studies.[3–5] Recently, targeting a standard cobalt-catalysed [2 + 2 + 2] cycloaddition to γ-spiro-γ-lactones, we have eventually reported the intriguing reactivity of enediynes featuring γ-alkylidenebutenolide compounds (Scheme 1). Due to the electronic specificities of the employed enediynes, a serendipitous Co(I)-mediated formal (2 + 2 + 3) cycloaddition reaction occurs allowing the highly regio- and diastereoselective formation of original cobalt(III) complexes. Preliminary computational studies have revealed an unusual mechanistic pathway relying on a fragmentation of the butenolide moiety (Scheme 1).[6] More precisely, after the oxidative coupling from $\mathbf{I^O}$, coordination of the alkene moiety would readily occur to give $\mathbf{II^O}$, due to its proximity to the metal centre, followed by the insertion step leading to $\mathbf{III^O}$. At this point, the mechanism differs from that of the classic [2 + 2 + 2] cycloaddition reaction. Instead of a reductive elimination step leading to the cobalt-complex-γ-spiro-γ-lactones $\mathbf{P2^O}$, a 7-membered ring would be generated through the formation

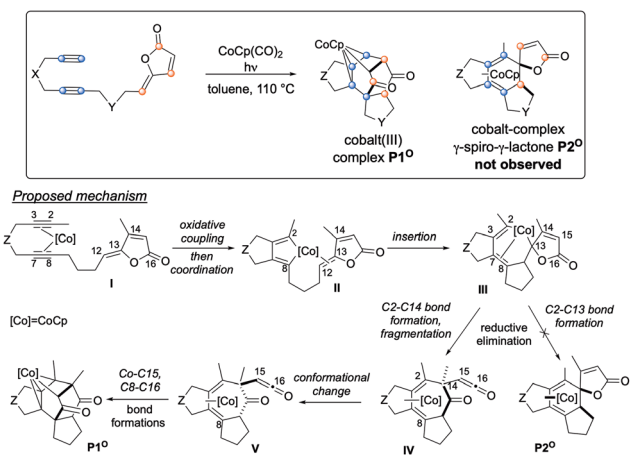

Scheme 1 Proposed mechanism for the cobalt-mediated formal (2 + 2 + 3) reaction.

Aix Marseille Univ, CNRS, Centrale Marseille, iSm2, Marseille, France.
E-mail: laurent.commeiras@univ-amu.f, paola.nava@univ-amu.fr, muriel.amatore@univ-amu.fr

†Electronic supplementary information (ESI) available: Additional computations, computational details, ^{1}H and ^{13}C NMR spectra of each compound, computed coordinates. See DOI: https://doi.org/10.1039/d3dt02291a

‡These authors contributed equally.

of the C2–C14 bond. This would cause the spontaneous fragmentation of the lactone, resulting into the formation of the crucial β-oxo-ketene intermediate $\mathbf{IV^O}$. From here, after a conformational change, a final step involving Co–C15 and C8–C16 bond formations would lead to the Co(III) complex $\mathbf{P1^O}$.

The molecular complexity of these unprecedented cobalt(III) complexes pushed us to perform further theoretical calculations by comparing intra- *versus* intermolecular approaches (Fig. 1a), and by computing the outcomes of a related Co(I)-mediated reaction employing γ-alkylidenebuterolactam as 2π partner, instead of γ-alkylidenebutenolide (Fig. 1b). The computational studies are systematically supported by experiments, which enable us to report the synthesis of new compounds.

Results and discussion

Intermolecular *vs.* intramolecular approaches

We first computationally studied the [2 + 2 + 2] cycloaddition reaction in an intermolecular fashion between the diyne derivative (2π + 2π partner) and the γ-alkylidenebutenolide (2π partner). The initial steps, which lead to the coordination of the alkene moiety to the cobaltacyclopentadiene, have been previously investigated for similar systems.[3,4,7] Notably, it has been already shown that the initial oxidative coupling between the two alkyne moieties leading to an intermediate of type **II** is preferred over a process implicating an oxidative coupling between a triple and a double bond.[3b] Therefore, the ΔG profiles (at 383.15 K) have been computed from intermediates of type **II**, obtained after the oxidative coupling and the coordination of the *exo*-cyclic double bond (Scheme 1). On the basis of Density Functional Theory calculations (DFT), it has been suggested that the final reductive elimination step of the [2 + 2 + 2] cycloaddition reaction would occur on a triplet potential energy surface. However, recent *ab initio* calculations reveal that the hopping on the triplet state surface is not necessary: the whole reaction can take place on the singlet potential energy surface.[5] Thus, no inter system crossing is to be invoked.

In the intermolecular reactivity, four coordination approaches are possible between the cobaltacyclopentadiene and the two double bonds of the γ-alkylidenebutenolide (Fig. 2): either the *exo*- and *endo*-approaches with the *exo*-cyclic double bond, or the *exo*- and *endo*-approaches with the *endo*-cyclic double bond. The energy of $\mathbf{II}_{exo}$ was chosen as reference.

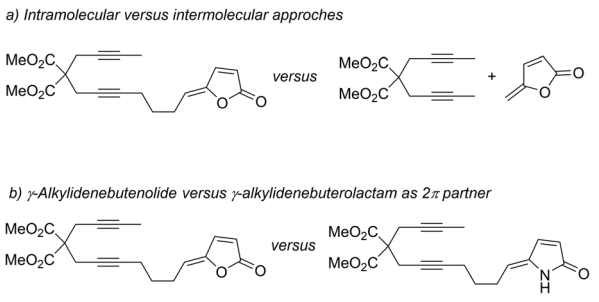

Fig. 1 Computational and experimental case studies.

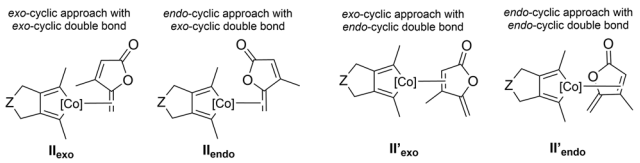

Fig. 2 Different coordination modes for the intermolecular approach.

From $\mathbf{II}_{exo}$ (Fig. 3 left), two regioselectivities can be envisioned for the insertion step of the *exo*-cyclic double bond: either the C2–C10 bond is formed to provide $\mathbf{III}_{exo1}$ (orange path), preventing the formation of the diketone product, or the C8–C9 bond is created to obtain $\mathbf{III}_{exo2}$ (blue path). By following the orange pathway, intermediate $\mathbf{III}_{exo1}$ evolves to the spirolactone $\mathbf{P2}_{exo}$ product through a transition state located at only 13.7 kcal mol^{-1}. The transition state leading to $\mathbf{III}_{exo2}$ is sterically more accessible and thus lower in energy (7.8 kcal mol^{-1}) than the one leading to $\mathbf{III}_{exo1}$ (10.5 kcal mol^{-1}). This accessibility results in intermediates that are significantly different in energy, with $\mathbf{III}_{exo2}$ more stable. From $\mathbf{III}_{exo2}$ two pathways can be considered: a reductive elimination step implicating the formation of the C2–C10 bond, would lead to the spirolactone $\mathbf{P2}_{exo}$ product, while the creation of the C2–C11 bond would cause the spontaneous fragmentation of the lactone. Two further steps are necessary to obtain the Co(III) complex $\mathbf{P1}_{exo}$. These two transition states are similar in energy, however barriers from $\mathbf{III}_{exo2}$ are quite high. Therefore, overall, even if the insertion step apparently would favour the process through $\mathbf{III}_{exo2}$, the approach through $\mathbf{III}_{exo1}$ is preferred, thus excluding the possibility to form $\mathbf{P1}_{exo}$.

In the pathway resulting from an *endo* approach (Fig. 3 right), two different insertion positions are again formally possible, with the creation of either the C2–C10 bond to $\mathbf{III}_{endo1}$ (orange path), or the C8–C9 bond to $\mathbf{III}_{endo2}$ (blue path). In both cases, only the spirolactone $\mathbf{P2}_{endo}$ product could be obtained. The obtention of the Co(III) complex would require the formation of the C2–C11 bond. However, in $\mathbf{III}_{endo2}$ the C11 is not correctly positioned face to C2. As for the *exo* approach, even if the insertion step is less accessible from the lactone side (orange path), the pathway through this approach is overall favoured, as the barrier for the reductive elimination is significantly lower.

We also computationally studied the coordination of the cobaltacyclopentadiene with the *endo*-cyclic double bond of the γ-alkylidenebutenolide ($\mathbf{II'}_{exo}$ and $\mathbf{II'}_{endo}$, Fig. 2). The system evolves towards the coordination of the cobaltacyclopentadiene with the *exo*-cyclic double bond of the 2π partner.

Our calculations demonstrate that the Co(III) complex is not accessible in the intermolecular version of the reaction. The overall costs to the γ-spiro-γ-lactone products $\mathbf{P2}_{exo}$ and $\mathbf{P2}_{endo}$ are similar: the highest transition states are located at 13.7 and 14.4 kcal mol^{-1} (less than 1 kcal mol^{-1} difference) for the *exo* and *endo* approaches, respectively, suggesting that the two products could be obtained. In both cases the insertion step through the lactone side (orange path) leads to an intermedi-

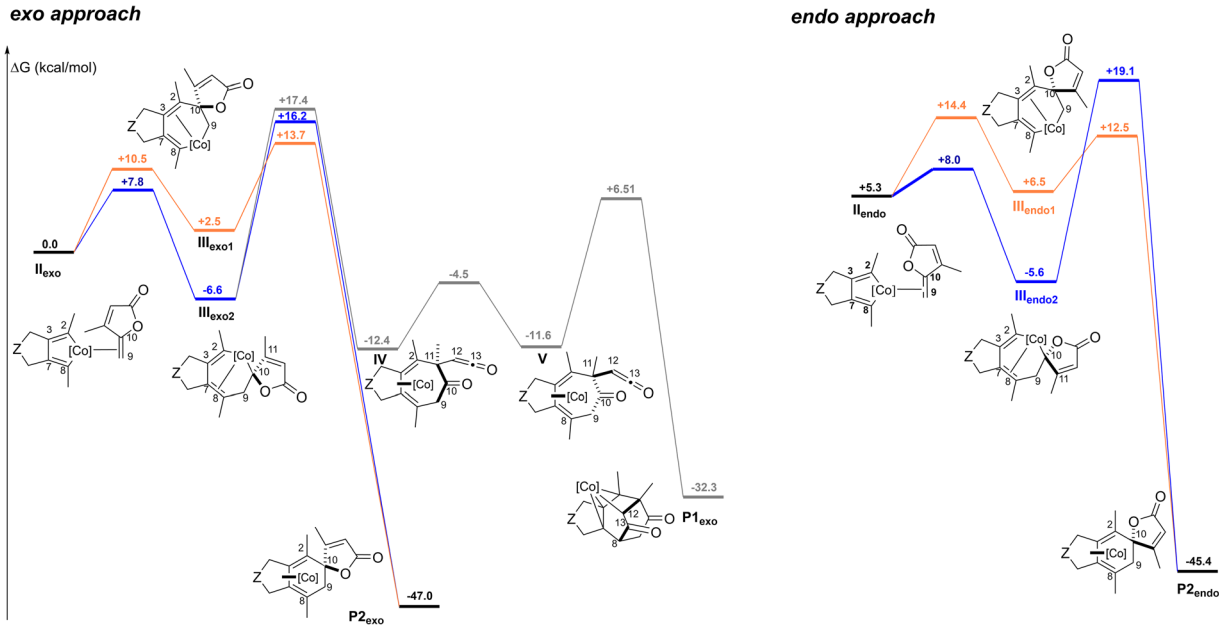

Fig. 3 Computed *exo*- and *endo*-pathways. Z = $C(CO_2Me)_2$, [Co] = CpCo. Δ*G* are computed at the TPSS-D3/def2-TZVP level (*T* = 383.15 K). Solvent effects are added as single point calculations with the COSMO implicit model (toluene).

ate with an accessible transition state for the reductive elimination step, preventing the possibility to form the β-oxo-ketene intermediate. This is not the case in the intramolecular approach. The presence of the tether between the diyne and the γ-alkylidenebutenolide facilitates the coordination of the alkene moiety by imposing an *exo*-like approach (Scheme 1). The resulting intermediate **III** has a connectivity similar to that of **III**$_{exo2}$, which differs from that of **III**$_{exo1}$. Importantly, only a connectivity as in **III**$_{exo2}$ allows to access to the Co(III) complex (see ESI† for details on the structures).

Experiments were then performed to corroborate the computational studies. Slightly reoptimized conditions developed for the intramolecular formation of Co(III) complex were applied for the intermolecular strategy (Scheme 2). The diyne partner **1a** (1 equiv.) and the γ-alkylidenebutenolide **2a** (3 equiv.) were exposed to a stoichiometric amount of $CpCo(CO)_2$ (1.2 equiv.) in toluene (0.25 mol L^{-1}) at 110 °C under irradiation (halogen 400 W) for one night. In these conditions, the formation of the predicted tricyclic spirolactone cobalt(I) complex **3a** was observed and isolated in 45% yield as a 1 : 0.2 mixture of two diastereomers. As the γ-alkylidenebutenolide employed displays two methyl substituents, it slightly differs from the lactone in Fig. 3. Calculations were therefore performed with the doubly substituted substrate, as well. The computed profiles (in the ESI†) are sensibly the same as those reported in Fig. 3, allowing to draw the same conclusion. The formation of the γ-spiro-γ-lactone cobalt complex is thus favoured over that of the Co(III) complex and the experimental result validates the conclusions of the theoretical study.

To enhance the synthetic potential of this tricyclic spirolactone cobalt complex **3a**, we then investigated its oxidative

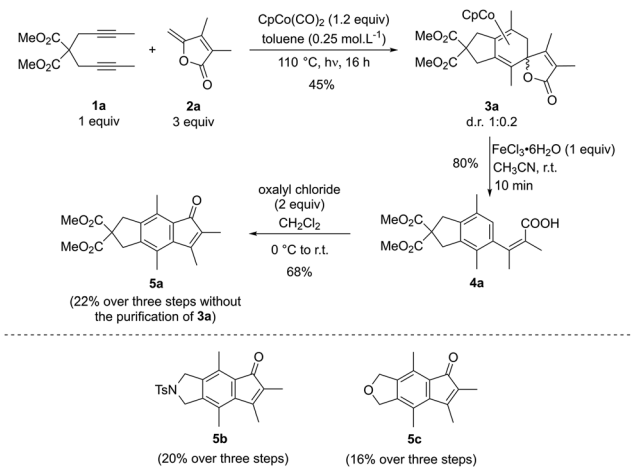

Scheme 2 Experimental evidence and post-functionalisation.

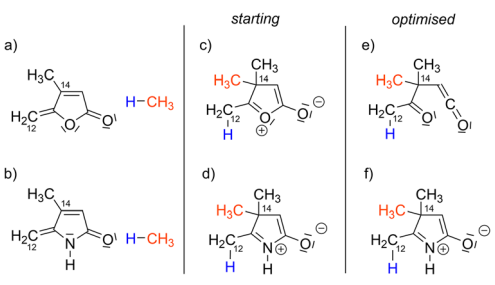

Fig. 4 Model reactivity. 'Starting' denotes the initial structures and 'Optimised' denotes the structure obtained after the geometry optimisations (PBE0/def2-TZVP).

demetallation. When **3a** is submitted to 1 equivalent of $FeCl_3{\cdot}6H_2O$ in acetonitrile, carboxylic acid **4a** was isolated in 80%, instead of the expected γ-spiro-γ-lactone compound. The formation of **4a** could be explained by a β-elimination step, after the decomplexation of the cobalt, which is favoured by the aromatisation of the 6-membered ring. It is worth noting that **4a** could be obtained in similar yield (33%), without the purification of the spirolactone cobalt complex **3a**. Finally, the indanone **5a** could be obtained in 68% yield when **4a** is treated with an excess of oxalyl chloride.

This sequential three-step synthesis was applied with two other diynes (Z = NTs and Z = O), providing the corresponding indenones **5b–5c** in 20 and 16% yields respectively.

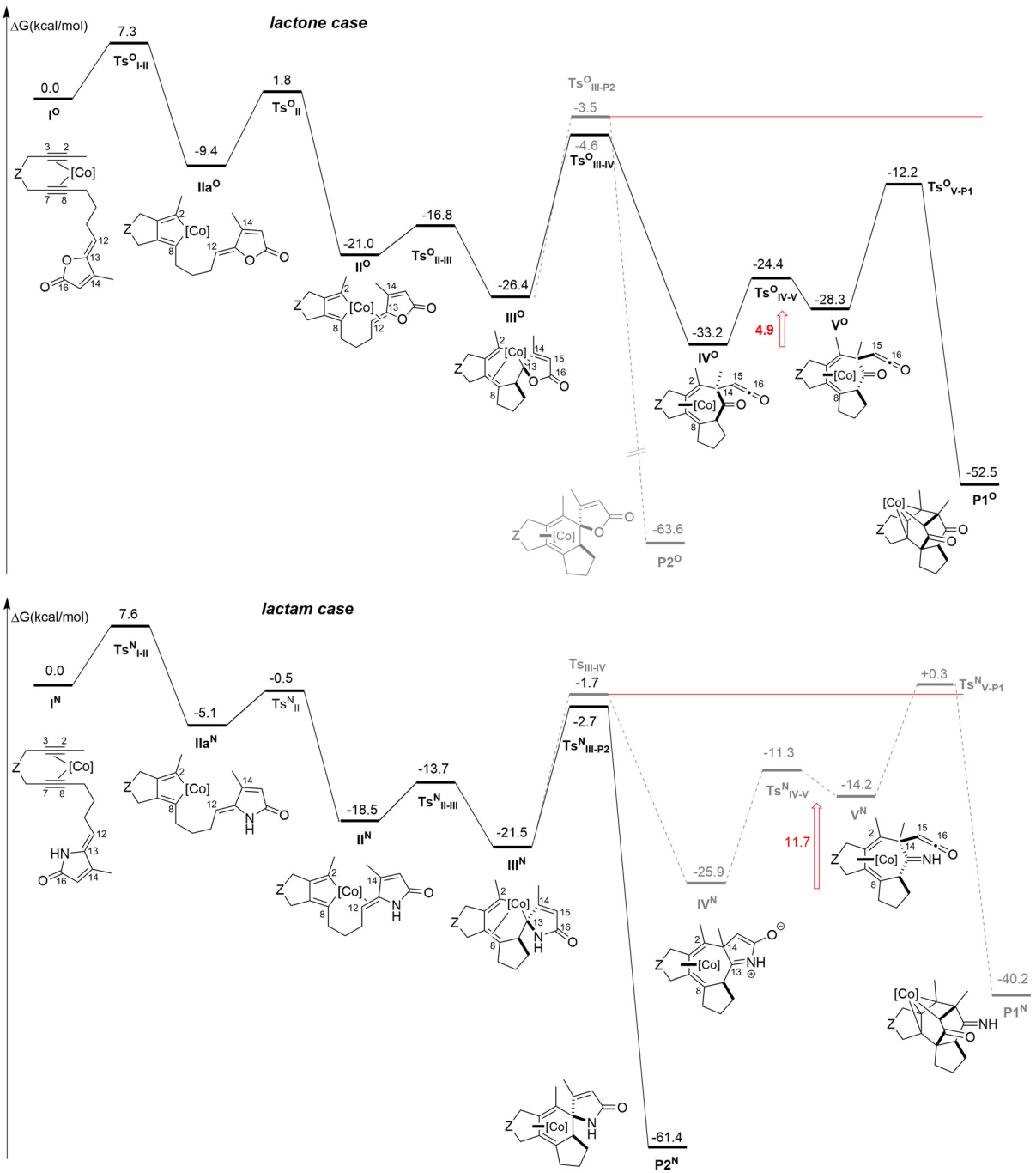

Fig. 5 Computed pathways for the possible intramolecular reactions. On top, lactone case, and lactam case at the bottom, Z = $C(C(O)OMe)_2$, [Co] = CpCo. Δ*G* are computed at the TPSS-D3/def2-TZVP level (*T* = 383.15 K). Solvent effects are added as single point calculations with the COSMO implicit model (toluene).

Lactone *vs.* lactam

Next, we investigated the outcome of the intramolecular cycloaddition reaction in the case where the lactone moiety is replaced by a lactam one. In the reactivity to the Co(III) complexes (Scheme 1), the insertion of the *exo*-cyclic double bond, the C12–C14 bond formation and the fragmentation of the lactone to the β-oxo-ketene are accompanied by the creation of two C–C σ-bonds, thus implying that two sp^2 carbon atoms, (C12 and C14, Scheme 1) are converted into sp^3 carbon atoms. To mimic this transformation, from sp^2 to sp^3 carbon atoms, two hypothetical structures were constructed by the addition of CH_4 (an H atom onto C12 and a CH_3 group onto C14) to both γ-alkylidenebutenolide and γ-alkylidenebuterolactam (Fig. 4a and b).

One the one hand, the Lewis structure of the lactone-derived system (Fig. 4c) displays an oxygen atom carrying a positive charge and the other oxygen atom carrying a negative charge. This charge separation suggests that it would not be stable. Indeed, a geometry optimisation was performed, and a spontaneous cleavage of the C–O bond is observed (Fig. 4e). On the other hand, the Lewis structure for the lactam-derived system (Fig. 4d) presents a charge separation, which is compatible with the electronegativity of the atoms, the nitrogen atom being formally charged plus and the oxygen minus. The geometry optimisation did not show the cleavage of the C–N bond (Fig. 4f). In this case, the fragmentation of the lactam ring is not spontaneous, which suggests that its transformation to β-imino-ketene moiety is less accessible than for the lactone moiety.

To verify this hypothesis, the mechanisms of the [2 + 2 + 2] cycloaddition reactions with a lactam moiety have been compared to those obtained with the lactone (Fig. 5). For clarity reason, we report on top of Fig. 5 the computed mechanism for the lactone case. The overall picture of this mechanism is the same as the one presented in Scheme 1 and previously reported, although ΔG values differ slightly, since we employ here a different level of calculations (see the computational details).[6] Moreover, we have detailed in the present work the coordination step from $\mathbf{IIa^O}$ to $\mathbf{II^O}$ through $\mathbf{Ts^O_{II}}$ that was not reported in our previous contribution.

Let us now describe the computed pathways for the lactam case. From $\mathbf{I^N}$, the pathway would be the following: the oxidative coupling takes place leading to $\mathbf{IIa^N}$ in a singlet state. The triplet state of $\mathbf{IIa^N}$ is lower in energy (ΔΔG = ΔG($^1\mathbf{IIa^N}$) – ΔG($^3\mathbf{IIa^N}$) = 5.2 kcal mol^{-1}), however the coordination of the alkene moiety to the metal is not possible on the triplet potential energy surface, while this coordination is readily accessible on the singlet state to $\mathbf{II^N}$. The insertion step would give $\mathbf{III^N}$.

From $\mathbf{III^N}$, the two pathways are considered. Notably, the transition state leading to the γ-spiro-γ-lactam cobalt complex ($\mathbf{Ts^N_{III\text{-}P2}}$ to $\mathbf{P2^N}$) is slightly lower than the one leading to the formation of the C2–C14 bond ($\mathbf{Ts^N_{III\text{-}IV}}$ to $\mathbf{IV^N}$). Interestingly and as predicted by the model (Fig. 4), the lactam ring does not open after $\mathbf{Ts^N_{III\text{-}IV}}$ to $\mathbf{IV^N}$. The following transformation, implying the fragmentation of the lactam moiety, would give an intermediate that is 11.7 kcal mol^{-1} higher than $\mathbf{IV^N}$ and the transition state leading to the hypothetical Co(III) product ($\mathbf{Ts^N_{V\text{-}P1}}$ to $\mathbf{P1^N}$) is even higher than $\mathbf{Ts^N_{III\text{-}IV}}$.

Finally, in the case of the lactam, the mechanisms of the [2 + 2 + 2] cycloaddition reaction is preferred over that leading to the $\mathbf{P1^N}$ product. The overall ΔG profiles differ from those computed for the lactone, where the 5-membered ring fragments immediately after the formation of the C2–C14 bond. Notably $\mathbf{V^O}$ would be only 4.9 kcal mol^{-1} higher in energy than $\mathbf{IV^O}$ and the last transition state ($\mathbf{Ts^O_{III\text{-}IV}}$) is lower than $\mathbf{Ts^O_{III\text{-}IV}}$ (Fig. 5).

The intramolecular [2 + 2 + 2] cycloaddition reaction of the ene-1,6-diyne containing a lactam scaffold, was then explored to validate the computational study (Scheme 3). The benchmark substrate **8** was prepared as a partially separable mixture of *E*/*Z* isomers.[8] After separation, each enriched diastereomer was submitted to the same reaction conditions as those for the intramolecular [2 + 2 + 2] cycloaddition reaction with a lactone scaffold (1.2 equiv. of $CpCo(CO)_2$ in toluene at 110 °C during 16 hours under irradiation (halogen 400 W)). Pleasingly, as predicted by the theoretical study, the cycloaddition reaction proceeded stereospecifically to give the desired γ-spiro-γ-lactam cobalt complexes **9-*cis*** and **9-*trans***, even with no full conversion. It is interesting to note an erosion of the stereospecificity of the cycloaddition reaction, which could be explained by the partial isomerization of the *exo*-cyclic double bond of the lactam moiety under the reaction conditions.

As the benchmark substrate **8** exists in the *Z* and *E* form, calculations were also performed on the latter. The computed mechanism shows that only a spiro product can be obtained from the *E* isomer, as detailed in the ESI.†

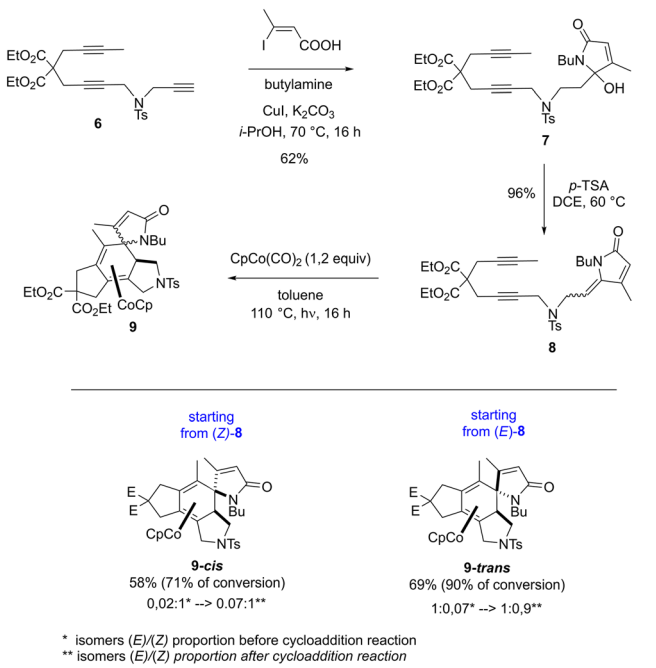

Scheme 3 Experimental evidence for the synthesis of γ-spiro-γ-lactam cobalt complexes **9**.

Conclusions

Two typologies of mechanisms are envisioned for cobalt cycloaddition reactions with γ-alkylidenebutenolide or γ-alkylidenebuterolactam as 2π partners, leading to either cobalt(III)- or cobalt(I)-spiro-complexes, the latter issued from standard [2 + 2 + 2] cycloadditions. The reductive elimination step, occurring on the singlet potential energy surface, is crucial for the selectivity: in one case the C–C bond formation leads to a cycloheptadiene that can further evolve to the cobalt (III) complex; in the other case, the generated C–C bond leads to the spiro product containing a cyclohexadiene. Calculations suggest that two ingredients are essential to obtain the cobalt (III) complex: the reaction needs to be performed in an intramolecular fashion, with a substrate carrying a lactone. Indeed, several coordination modes of the 2π partner to the metal are possible in the intermolecular case, while the molecular link joining the lactone to the diyne moiety imposes the structural motif favourable to the formation of the cycloheptadiene in the intramolecular approach. Furthermore, the comparison between the lactam and lactone reveals that the lactam does not fragment after the reductive elimination, while the lactone breaks spontaneously to generate the ketene intermediate, which reacts further. Finally, experimental studies have confirmed the theoretical predictions: spiro compounds were obtained through [2 + 2 + 2] cycloaddition reactions starting from lactone substrates in an intermolecular fashion and from lactam derivatives in an intramolecular way.

Experimental

Computational details

Density functional theory calculations were performed using the TURBOMOLE program package.[9] The TPSS functional was employed to obtain the mechanistic profiles, together with the empirical dispersion corrections D3 (TPSS-D3).[10] The basis set is of def2-TZVP quality for all atoms and the corresponding auxiliary basis sets for the RI treatment were selected.[11] Solvent effects are added as single point calculations with the COSMO implicit model (toluene).[12]

The mechanism for the lactone substrate in Fig. 5 was newly calculated to provide comparable results with those proposed in this contribution. Results between calculations performed at the BP86-D3 level (the method used in our preliminary work)[6] and those obtained at the TPSS-D3 level here reported are almost identical. However, we decided to systematically employ the TPSS-D3 functional because it belongs to the *meta*-GGA functional family, which represents an improvement over the GGA functionals (as BP86). The TPSS functional is a general purpose functional that works well for transition metal complexes (notably 3d metals)[10f] and provides, as well, good results on the energetics of cobalt complexes, when comparing singlet and triplet states. Singlet and triplet potential energy surfaces get close for some intermediates of the cobalt-catalysed or mediated cycloaddition reactions, although we focused in this work on steps occurring on the singlet potential energy surface. We employ here the TPSS-D3 functional because it provides the triplet *vs.* singlet energy ordering predicted by *ab initio* calculations, whereas methods as B3LYP or PBE0 tend to over-stabilise triplets in some cases, in particular for the insertion intermediate.[5]

The lactam reaction pathway was computed by three different DFT methods (BP86-D3,[10a,b,e,13] TPSS-D3, PBE0-D3 functionals,[10a,b,e,14] def2-TZVP basis set, see ESI†). Importantly, all computations deliver the same qualitative picture, predicting that the pathway to the Co(III) complex is less favoured than the one to the spirocyclic lactam Co(I) complex. However, relative energies are somewhat sensitive to the method used, notably the difference in energy between $\mathbf{III^N}$ and $\mathbf{II^N}$ is of −3.0 kcal mol^{-1} at the TPSS-D3 level and decreases to −10.3 kcal mol^{-1} at the PBE0-D3 level. We have then checked that the TPSS-D3 method would provide reasonable results: we considered the model systems for the cobaltacyclopentadiene coordinated by an alkene, $\mathbf{II^{mod}}$, and for the intermediate following the insertion, $\mathbf{III^{mod}}$. The energy differences ($\Delta E = E_{\mathbf{IIImod}} - E_{\mathbf{IImod}}$, without ZPE, gas phase) between these complexes, computed at DFT (BP86-D3, TPSS-D3, PBE0-D3 functionals, def2-TZVP basis set) and CCSD(T) levels, are reported in Table 1. CCSD(T) calculations, performed with the MOLPRO program package, are single point calculations on TPSS structures and employ the aug-cc-pwCVTZ-DK, cc-pVTZ-DK and cc-pVDZ-DK basis sets for Co, C and H, respectively. Results from TPSS-D3 and BP86-D3 are close to the CCSD(T) value (within 1.6 kcal mol^{-1}), whereas the PBE0 method predicts the insertion intermediate somewhat too stable than $\mathbf{II^{mod}}$. We concluded that the TPSS-D3 calculations would give a more accurate global picture of the treated mechanisms than the hybrid GGA (Generalized Gradient Approximation) PBE0 functional in these cases.

General

^{1}H Nuclear Magnetic Resonance (NMR) spectra were recorded using an internal deuterium lock at ambient temperatures on the following instruments: Bruker AC400 (400 MHz) and Bruker AC300 (300 MHz). The internal references of ^{1}H 7.26 was used for the residual protons in $CDCl_3$. Data are presented as follows: chemical shift (in ppm), integration, interpretation,

Table 1 Computed differences in energy between $\mathbf{III^{mod}}$ and $\mathbf{II^{mod}}$ ($\Delta E = E_{\mathbf{IIImod}} - E_{\mathbf{IImod}}$, singlet state)

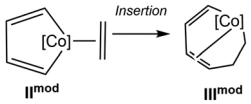

Method	ΔE (kcal mol^{-1})
CCSD(T)	−8.0
BP86-D3	−6.6
TPSS-D3	−6.4
PBE0-D3	−13.1

multiplicity (s = singlet, d = doublet, t = triplet, q = quartet, quintet = quin, m = multiplet, dd = doublet of doublet, dt = doublet of triplet, br = broad) and coupling constant (*J* in Hz). ^{13}C NMR spectra were recorded on a Bruker AC400 (101 MHz) and a Bruker AC300 (75 MHz) spectrometers with complete proton decoupling. Chemical shifts were reported in ppm from the internal solvent signal (peak at 77.16 ppm in the case of $CDCl_3$).

Infra-red spectra were recorded on a Bruker VERTEX70 Fourier transform infrared spectrometer fitted with a single reflection diamond ATR Bruker A222 accessory. The measurements were done for pure samples. For each individual spectrum, about 30 scans were averaged at 4 cm^{-1} resolution. The diamond crystal without sample served as reference. All the system was purged with dry air. The identification of peaks was done with the standard method proposed in OPUS 6.0 software. Wavelengths of maximum absorbance (max) are quoted in cm^{-1}.

High resolution MS experiments were performed with a QSTAR Elite mass spectrometer (Applied Biosystems SCIEX) or a SYNAPT G2 HDMS mass spectrometer (Waters) equipped with an electrospray ionization source operated in the positive ion mode. In this hybrid instrument, ions were measured using an orthogonal acceleration time-of-flight (oa-TOF) mass analyzer.

Analytical thin layer chromatography (TLC) was carried out on Merck® Kieselgel 60 F254 plates and achieved under a 254 nM UV light, visualized with a $KMnO_4$ solution or anisaldehyde solution.

Synthesis

Compound 3a. The diyne **1a** (30 mg, 0.127 mmol, 1 equiv.) and the lactone **2a** (47 mg, 0.38 mmol, 3 equiv.) were charged in a Schlenk tube under inert atmosphere. Dry toluene (0.5 mL) was then added, and the solution was degassed twice at −78 °C. Dicarbonylcyclopentadienylcobalt (20 μL, 0.15 mmol, 1.2 equiv.) was then added thanks to a syringe and the Schlenk tube was sealed. The mixture was stirred under irradiation (halogen 400 W) during 16 hours at 110 °C then concentrated *in vacuo*. The crude was purified by flash chromatography on silica gel (PE/AcOEt 9 : 1) to give **3a** as 1/0.2 mixture of diastereomers (28 mg, 45% yield). Major diastereomer: mp 159 °C; ^{1}H NMR (300 MHz, chloroform-*d*) δ 0.89 (s, 3H), 1.11 (br d, *J* = 15.8 Hz, 1H), 1.29 (br s, 3H), 1.36 (br q, *J* = 1.0 Hz, 3H), 1.69 (br q, *J* = 1.0 Hz, 3H), 1.92 (d, *J* = 15.8 Hz, 1H), 3.13 (d, *J* = 16.4 Hz, 1H), 3.17 (d, *J* = 16.4 Hz, 1H), 3.67 (d, *J* = 16.4 Hz, 1H), 3.69 (d, *J* = 16.4 Hz, 1H), 3.80 (s, 3H), 3.89 (s, 3H), 4.48 (s, 5H); ^{13}C NMR (75 MHz, chloroform-*d*) δ 8.5, 10.3, 16.4, 23.5, 39.0, 39.4, 44.2, 53.2, 53.4, 55.9, 56.2, 60.2, 82.8 (5C), 94.5, 94.7, 94.9, 122.5, 161.1, 172.4, 173.0, 174.5; HRMS (ESI-MS) calcd for $C_{25}H_{30}O_6Co^+$ $[M + H]^+$ 485.1369, found 485.1364; IR ν_{max}/cm^{-1} 2956, 1735, 1436, 1257, 1199, 116.

Compound 4a. To a solution of **3a** (20 mg, 0.041 mmol, 1 equiv.) in acetonitrile (1 mL) was added $FeCl_3{\cdot}H_2O$ (11 mg, 0.041 mmol, 1 equiv.) at room temperature. The reaction mixture was stirred for 5 minutes, filtered through a pad of Celite and concentrated *in vacuo*. The crude was purified by flash chromatography on silica gel (PE/AcOEt from 9 : 1 to 8 : 2) to give **4a** (12 mg, 80% yield). Mp 171 °C; ^{1}H NMR (300 MHz, chloroform-*d*) δ 1.99 (br q, *J* = 1.1 Hz, 3H), 2.02 (br q, *J* = 1.1 Hz, 3H), 2.03 (s, 3H) 2.17 (s, 3H), 3.54 (s, 4H), 3.75 (s, 3H), 3.77 (s, 3H), 6.61 (s, 1H), *OH not observed*; ^{13}C NMR (75 MHz, chloroform-*d*) δ 15.8, 15.9, 18.7, 23.3, 39.9, 40.3, 53.1 (2C), 59.6, 125.0, 126.6, 127.1, 130.9, 137.6, 139.2, 142.3, 147.8, 171.2, 172.4, 172.7; HRMS (ESI-MS) calcd for $C_{20}H_{28}NO_6^+$ $[M + NH_4]^+$ 378.1911, found 378.1914; IR ν_{max}/cm^{-1} 2010, 1726, 1658, 1433, 1280, 1255, 1190, 1155, 1076, 1057.

Compound 5a. To a solution of **4a** (10 mg, 0.027 mmol, 1 equiv.) in dry DCM (0.3 mL) was added oxalyl chloride (2.6 μL, 0.054 mmol, 2 equiv.) at 0 °C under argon. The resulting solution was stirred at 0 °C for 1 hour then at room temperature for 2 hours. The solvent was removed *in vacuo* and the crude was purified by flash chromatography on silica gel (PE/AcOEt 8 : 2) to give **5a** (6.5 mg, 68% yield). Mp 198 °C; ^{1}H NMR (400 MHz, chloroform-*d*) δ 1.74 (br q, *J* = 1.6 Hz, 3H), 2.23 (br q, *J* = 1.6 Hz, 3H), 2.31 (s, 3H), 2.40 (s, 3H), 3.49 (s, 2H), 3.51 (s, 2H), 3.77 (s, 6H); ^{13}C NMR (101 MHz, chloroform-*d*) δ 7.6, 13.7, 15.8, 16.0, 39.3, 40.4, 53.2 (2C), 59.2, 125.2, 127.8, 130.9, 131.4, 139.8, 143.2, 144.9, 154.1, 172.2 (2C); 199.4; HRMS (ESI-MS) calcd for $C_{20}H_{23}O_5^+$ $[M + H]^+$ 343.1540, found 343.1541; IR ν_{max}/cm^{-1} 1734, 1693, 1429, 1265, 1065, 1159, 1080, 1049.

General procedure for the three steps synthesis of indenones 5. The diyne **1** (1 equiv.) and the lactone **2** (3 equiv.) were charged in a Schlenk tube under inert atmosphere. Dry toluene (0.25 mol L^{-1}) was then added, and the solution was degassed twice at −78 °C. Dicarbonylcyclopentadienylcobalt (1.2 equiv.) was then added thanks to a syringe and the Schlenk tube was sealed. The mixture was stirred under irradiation (halogen 400 W) during 16 hours at 110 °C then concentrated *in vacuo*. The cobalt complex was directly used in the next step. To a solution of the intermediate in acetonitrile (0.04 mol L^{-1}) was added $FeCl_3{\cdot}H_2O$ (1 equiv.). After 10 min of stirring, the mixture was filtered through a pad of silica then concentrated. The crude was purified by flash chromatography on silica gel. To a solution of carboxylic acid in dry DCM (0.09 mol L^{-1}) was added oxalyl chloride (2 equiv.) at 0 °C under argon. The resulting solution was stirred at 0 °C for 1 hour then at room temperature for 2 hours. The solvent was removed *in vacuo* and the crude was purified by flash chromatography on silica gel.

Compound 5b. The desired product was obtained according to the general procedure starting from 47 mg (0.38 mmol) of lactone **1a** and 35 mg of diyne **2b** (0.127 mmol). **5b** (5.1 mg, 20% yield) was purified by flash chromatography on silica gel (PE/AcOEt 9 : 1 to 8 : 2). Mp 140 °C; ^{1}H NMR (300 MHz, chloroform-*d*) δ 1.74 (br q, *J* = 1.3 Hz, 3H), 2.22 (br q, *J* = 1.3 Hz, 3H), 2.24 (s, 3H), 2.32 (s, 3H), 2.41 (s, 3H), 4.45–4.61 (m, 4H), 7.33 (d, *J* = 8.5 Hz, 2H), 7.78 (d, *J* = 8.5 Hz, 2H). ^{13}C NMR (75 MHz, $CDCl_3$) δ 7.5, 13.5, 15.6, 15.9, 21.7, 53.4, 54.1, 123.7, 127.7 (2C), 128.4, 129.4, 130.1 (2C), 132.0, 134.1, 136.3, 141.1, 143.8, 143.9, 153.8, 198.7; HRMS (ESI-MS) calcd for $C_{22}H_{24}NO_3S$

$[M + H]^+$ 382.1471 found 382.1468; IR ν_{max}/cm^{-1} 2360, 1689, 1631, 1352, 1161, 1099.

Compound 5c. The desired product was obtained according to the general procedure starting from 47 mg (0.38 mmol) of lactone **1a** and 35 mg of diyne **2c** (0.127 mmol). **5c** (10 mg, 16% yield) was purified by flash chromatography on silica gel (PE/AcOEt 95 : 5 to 8 : 2). ^{1}H NMR (300 MHz, chloroform-*d*) δ 1.76 (br q, J = 1.3 Hz, 3H), 2.25 (br q, J = 1.3 Hz, 3H), 2.27 (s, 3H), 2.37 (s, 3H), 5.07 (s, 4H); ^{13}C NMR (75 MHz, chloroform-*d*) δ 7.5, 13.9, 15.9, 16.0, 73.9, 74.3, 122.7, 128.4, 128.5, 131.7, 139.1, 143.8, 144.2, 153.9, 199.1; HRMS (ESI-MS) calcd for $C_{15}H_{17}O_2^+$ $[M + H]^+$ 229.1223, found 229.1223; IR ν_{max}/cm^{-1} 2922, 1685, 1471, 1375, 1055, 906.

Compound 7. To a solution of (*Z*)-3-substituted-3-iodoprop-2-enoic acid derivative (90 mg, 0.42 mmol, 1 equiv.) in i-PrOH (1.5 mL) in an oven-dried-Schlenk tube was added K_2CO_3 (117 mg, 0.84 mmol, 2 equiv.). The suspension was stirred for 10 minutes under argon. The mixture was then degassed at −78 °C for 2 × 10 min and the reaction vessel was backfilled with argon. After warming to room temperature, triyne **6**[6] (200 mg, 0.42 mmol, 1 equiv.), butylamine (125 µL, 1.27 mmol, 3 equiv.) and finally CuI (16 mg, 0.085 mmol, 0.2 equiv.) were added. The mixture was then rapidly degassed and was backfilled with argon. The sealed Schlenk tube was stirred for 16 hours at 70 °C. The reaction mixture was cooled to 0 °C, then quenched by the addition of aqueous saturated solution of NH_4Cl and was stirred for further 15 min. The mixture was filtered through a pad of Celite. The aqueous phase was extracted with EtOAc. The combined organic layers were washed with brine, dried over Na_2SO_4, filtered and concentrated *in vacuo*. The crude was purified by flash chromatography on silica gel (PE/AcOEt from 9 : 1 to 8 : 2) to give the corresponding hydroxylactam **7** (166 mg, 62% yield). ^{1}H NMR (300 MHz, chloroform-*d*) δ 0.94 (t, J = 7.3 Hz, 3H), 1.24 (q, J = 7.0 Hz, 3H), 1.25 (q, J = 7.0 Hz, 3H), 1.35 (sixt, J = 7.5 Hz, 2H), 1.57–1.70 (m, 2H), 1.74 (br t, J = 2.5 Hz, 3H), 2.01 (br d, J = 1.6 Hz, 3H), 2.11–2.21 (m, 1H), 2.28–2.38 (m, 1H), 2.42 (s, 3H), 2.64–2.82 (m, 6H), 3.03–3.13 (m, 1H), 3.40–3.50 (m, 1H), 3.95–4.2 (m, 6H), 5.76 (br q, J = 1.6 Hz, 1H), 7.29 (d, J = 8.4 Hz, 2H), 7.61 (d, J = 8.4 Hz, 2H), *OH not observed*; ^{13}C NMR (75 MHz, $CDCl_3$) δ 3.6, 12.1, 13.9, 14.2 (2C), 20.7, 21.7, 22.9, 23.1, 31.6, 32.5, 38.0, 38.8, 42.0, 56.6, 62.1 (2C), 73.0, 76.6, 79.3, 80.7, 91.9, 123.1, 127.5 (2C), 129.9 (2C), 135.9, 143.9, 158.8, 169.0 (2C), 169.8; HRMS (ESI-MS) calcd for $C_{33}H_{45}N_2O_8S$ $[M + H]^+$ 629.2891 found 629.2892; IR ν_{max}/cm^{-1} 2954, 1732, 1683, 1355, 1327, 1290, 1197, 1153, 1087, 1047, 723, 663, 576.

Compounds 8. To a solution of hydroxylactam **7** (320 mg, 0.509 mmol, 1 equiv.) in dichloroethane (1 mL) was added *p*-TSA (29 mg, 0.152 mmol, 0.3 equiv.). The mixture was stirred for 1 hour at 60 °C then quenched with water. The aqueous phase was extracted with dichloromethane. The combined organic layers were dried over Na_2SO_4 filtered and concentrated *in vacuo.* The crude composed of a 1/0.6 mixture of (*E*/*Z*)-**8** was purifed by flash chromatography on silica gel (PE : EtOAc 8 : 2) to give both enriched diastereomers (m ((*Z*)-**8** + (*E*)-**8**) = 299 mg, 96% yield). HRMS (ESI-MS) calcd for $C_{33}H_{43}N_2O_7S$ $[M + H]^+$ 611.2786 found 611.2789.

(*Z*)-**8**: ^{1}H NMR (300 MHz, chloroform-*d*) δ 0.91 (t, J = 7.3 Hz, 3H), 1.21 (t, J = 7.1 Hz, 6H), 1.25–1.37 (m, 2H), 1.45–1.56 (m, 2H), 1.72 (br t, J = 2.4 Hz, 3H), 1.97 (br d, J = 1.5 Hz, 3H), 2.43 (s, 3H), 2.67 (br q, J = 2.4 Hz, 2H), 2.73 (br t, J = 2.1 Hz, 2H), 3.69 (dd, J = 7.3 Hz, 2H), 4.08–4.26 (m, 8H), 4.98 (t, J = 7.0 Hz, 1H), 5.85 (br q, J = 1.5 Hz, 1H), 7.32 (d, J = 7.9 Hz, 2H), 7.70 (d, J = 7.9 Hz, 2H); ^{13}C NMR (75 MHz, $CDCl_3$) δ 3.6, 12.4, 13.9, 14.1 (2C), 20.0, 21.7, 22.8, 23.0, 32.0, 37.3, 40.7, 43.4, 56.6, 62.0 (2C), 73.0, 76.0, 79.2, 81.3, 104.8, 120.5, 127.8 (2C), 129.8 (2C), 136.0, 141.9, 144.0, 148.5, 168.9 (2C), 170.9; IR ν_{max}/cm^{-1} 1728, 1357, 1296, 1199, 1159, 1089, 1051, 894, 752, 655.

(*E*)-**8**: ^{1}H NMR (300 MHz, chloroform-*d*) δ 0.89 (t, J = 7.2 Hz, 3H), 1.20 (t, J = 7.1 Hz, 6H), 1.18–1.30 (m, 2H), 1.34–1.47 (m, 2H), 1.72 (t, J = 2.5 Hz, 3H), 2.29 (br d, J = 1.6 Hz, 3H), 2.43 (s, 3H), 2.67 (br q, J = 2.5 Hz, 2H), 2.74 (br t, J = 2.3 Hz, 2H), 3.44 (t, J = 7.2 Hz, 2H), 4.05–4.19 (m, 6H), 4.23 (d, J = 7.6 Hz, 2H), 5.14 (t, J = 7.6 Hz, 1H), 5.93 (br q, J = 1.6 Hz, 1H), 7.28–7.37 (d, J = 7.9 Hz, 2H), 7.64–7.76 (d, J = 7.9 Hz, 2H); ^{13}C NMR (75 MHz, $CDCl_3$) δ 3.5, 13.9, 14.1 (2C), 16.8, 20.2, 21.7, 22.8, 23.0, 30.8, 36.9, 38.6, 43.2, 56.5, 61.9 (2C), 73.0, 76.1, 79.1, 81.1, 107.3, 124.7, 127.7 (2C), 129.8 (2C), 136.2, 142.2, 143.9, 145.7, 168.8 (2C), 168.9; IR ν_{max}/cm^{-1} 2960, 1743, 1689, 1352, 1205, 1159, 1085, 1057.

Compound 9-*cis*. Enriched compound (*Z*)-**8** (*Z*/*E*: 1/0.02, 23 mg, 0.037 mmol, 1 equiv.) was charged in a Schlenk tube under inert atmosphere. Dry toluene (1.1 mL) was then added, and the solution was degassed twice at −78 °C. Dicarbonylcyclopentadienylcobalt (6 µL, 0.045 mmol, 1.2 equiv.) was added to the solution and the Schlenk tube was sealed. The mixture was heated at 110 °C under irradiation (halogen 400 W) for 16 hours then concentrated *in vacuo.* The crude was purified by flash chromatography on silica gel (PE/AcOEt 6/4) to give 1 : 0.07 inseparable mixture of **9-*cis*** and **9-*trans*** (16 mg, 58% yield, 62% yield, 71% of conversion). ^{1}H NMR (300 MHz, chloroform-*d*) δ 0.69 (s, 3H), 1.17 (t, J = 6.9 Hz, 3H), 1.29 (t, J = 7.1 Hz, 3H), 1.32–1.36 (m, 7H), 1.41–1.70 (m, 4H), 2.20–2.35 (m, 1H), 2.45 (s, 3H), 3.10–3.66 (m, 9 H), 4.12 (s, 5H), 4.25 (q, J = 7.1 Hz, 2H), 4.35 (br q, J = 7.1 Hz, 2H), 5.59 (br q, J = 1.6 Hz, 1H), 7.42 (d, J = 8.1 Hz, 2H), 7.82 (d, J = 8.1 Hz, 2H); ^{13}C NMR (75 MHz, chloroform-*d*) δ 12.6, 14.2, 14.3 (2C), 17.5, 21.6, 21.7, 30.2, 39.4, 40.1, 44.0, 48.7, 51.4, 53.6, 59.4, 60.5, 62.4, 62.6, 63.7, 84.0 (5C), 89.8, 95.2, 121.4, 127.9 (2 C), 130.0 (2 C), 134.0, 144.2, 160.6, 171.7, 172.2, 173.4 (*one quaternary C carbon is in CDCl$_3$ peaks*); HRMS (ESI-MS) calcd for $C_{38}H_{48}N_2O_7SCo$ $[M + H]^+$ 735.2509, found 735.2509; IR ν_{max}/cm^{-1} 2960, 2927, 1726, 1685, 1342, 1246, 1161, 1101, 1045, 1008, 802, 673.

Compound 9-*trans*. Enriched compound (*E*)-**8** (*E*/*Z*: 1/0.07, 35 mg, 0.057 mmol, 1 equiv.) was charged in a Schlenk tube under inert atmosphere. Dry toluene (1.6 mL) was then added, and the solution was degassed twice at −78 °C. Dicarbonylcyclopentadienylcobalt (9 µL, 0.069 mmol, 1.2 equiv.) was added to the solution and the Schlenk tube was sealed. The mixture was heated at 110 °C under irradiation

(halogen 400 W) for 16 hours then concentrated *in vacuo*. The crude was purified by flash chromatography on silica gel (PE/AcOEt 6/4) to give 1 : 0.09 inseparable mixture of **9-*cis*** and **9-*trans*** (29 mg, 69% yield, 90% of conversion). ^{1}H NMR (300 MHz, chloroform-*d*) δ 0.77 (s, 3H), 0.83 (t, J = 7.0 Hz, 3H), 1.09–1.20 (m, 3H), 1.20–1.27 (m, 1H), 1.30 (t, J = 7.1 Hz, 3H), 1.36 (t, J = 7.1 Hz, 3H), 1.41–1.51 (m, 1H), 2.26–2.38 (m, 1H), 2.43 (s, 3H), 2.53 (br d, J = 1.5 Hz, 3H), 2.60–2.73 (m, 1H), 3.08 (d, J = 17.0 Hz, 1H), 3.16 (br s, 2H), 3.34 (br dd, J = 7.8 and 8.6 Hz, 1H), 3.45 (d, J = 17.0 Hz, 1H), 3.55 (d, J = 17.0 Hz, 1H), 3.68–3.73 (m, 1H), 3.73 (d, J = 17.0 Hz, 1H), 4.23 (s, 5H), 4.23–4.39 (m, 4H), 5.82 (br q, J = 1.5 Hz, 1H), 7.39 (d, J = 8.3 Hz, 2H), 7.75 (d, J = 8.3 Hz, 2H); ^{13}C NMR (75 MHz, chloroform-*d*) δ 13.9, 14.2, 14.3, 17.8, 17.9, 20.5, 21.7, 30.8, 39.3, 39.7, 39.8, 49.4, 50.9, 53.2, 56.5, 59.8, 60.1, 62.4, 62.6, 77.5, 84.0 (5C), 89.7, 95.2, 126.3, 127.7 (2 C), 130.0 (2C), 134.1, 144.1, 158.2, 169.6, 171.7, 171.9; HRMS (ESI-MS) calcd for $C_{38}H_{48}N_2O_7SCo$ $[M + H]^+$ 735.2509, found 735.2509; IR ν_{max}/cm^{-1} 1734, 1687, 1348, 1259, 1182, 1151, 1093, 1051, 1010, 823, 673.

Conflicts of interest

There are no conflicts to declare.

Acknowledgements

L. C and M. D. thanks the French Research Ministry, Aix-Marseille University and CNRS for financial support.

References

1 Selected references: (*a*) W. Reppe, O. Schichting, K. Klager and T. Toepel, *Justus Liebigs Ann. Chem.*, 1948, **560**, 1–92; (*b*) J. M. Halford-McGuff, A. M. Z. Slawin and A. J. B. Watson, *ACS Catal.*, 2023, **13**, 3463–3470; (*c*) P. Matton, S. Huvelle, M. Haddad, P. Phansavath and V. Ratovelomanana-Vidal, *Synthesis*, 2022, **54**, 4–32; (*d*) A. Lledo, A. Pla-Quintana and A. Roglans, *Chem. Soc. Rev.*, 2016, **45**, 2010–2023; (*e*) Y. Sato and Y. Obora, *Eur. J. Org. Chem.*, 2015, 5041–5054; (*f*) S. Okamoto and Y. Sugiyama, *Synlett*, 2013, 1044–1060; (*g*) *Transition-Metal-Mediated Aromatic Ring Construction*, ed. K. Tanaka, John Wiley & Sons, Hoboken, 2013; (*h*) Y. Shibata and K. Tanaka, *Synthesis*, 2012, 323–350; (*i*) K. Tanaka, *Heterocycles*, 2012, **85**, 1017–1043; (*j*) D. L. J. Broere and E. Ruijter, *Synthesis*, 2012, 2639–2672; (*k*) G. Domínguez and J. Pérez-Castells, *Chem. Soc. Rev.*, 2011, **40**, 3430–3444; (*l*) M. R. Shaaban, R. El-Sayed and A. H. M. Elwahy, *Tetrahedron*, 2011, **67**, 6095–6130; (*m*) N. Wedding and M. Hapke, *Chem. Soc. Rev.*, 2011, **40**, 4525–4538; (*n*) D. Leboeuf, V. Gandon and M. Malacria, in *Handbook of Cyclization Reactions*, ed. S. Ma, Wiley-VCH, Weinheim, 2009; (*o*) N. Agenet, V. Gandon, O. Buisine, F. Slowinski and M. Malacria, *Organic Reactions*, ed. T. V. RajanBabu, Wiley, Hoboken, NJ, 2007; (*p*) V. Gandon, C. Aubert and M. Malacria, *Chem. Commun.*, 2006, 2209–2217.

2 G. Domínguez and J. Pérez-Castells, *Chem. – Eur. J.*, 2016, **22**, 6720–6739.

3 (*a*) D. Leboeuf, L. Iannazzo, A. Geny, M. Malacria, K. P. C. Vollhardt, C. Aubert and V. Gandon, *Chem. – Eur. J.*, 2010, **16**, 8904–8913; (*b*) V. Gandon, N. Agenet, K. P. C. Vollhardt, M. Malacria and C. Aubert, *J. Am. Chem. Soc.*, 2006, **128**, 8509–8520; (*c*) N. Agenet, V. Gandon, K. P. C. Vollhardt, M. Malacria and C. Aubert, *J. Am. Chem. Soc.*, 2007, **129**, 8860–8871.

4 A. Roglans, A. Pla-Quintana and M. Solà, *Chem. Rev.*, 2021, **121**, 1894–1979.

5 L. Chaussy, D. Hagebaum-Reignier, S. Humbel and P. Nava, *Phys. Chem. Chem. Phys.*, 2022, **24**, 21841–21852.

6 M. Delorme, A. Punter, R. Oliveira, C. Aubert, Y. Carissan, J.-L. Parrain, M. Amatore, P. Nava and L. Commeiras, *Dalton Trans.*, 2019, **48**, 15767–15771.

7 (*a*) A. A. Bengali, R. G. Bergman and C. B. Moore, *J. Am. Chem. Soc.*, 1995, **117**, 3879–3880; (*b*) P. E. M. Siegbahn, *J. Am. Chem. Soc.*, 1996, **118**, 1487–1496; (*c*) A. A. Dahy and N. Koga, *Bull. Chem. Soc. Jpn.*, 2005, **78**, 781–791; (*d*) A. A. Dahy, C. H. Suresh and N. Koga, *Bull. Chem. Soc. Jpn.*, 2005, **78**, 792–803.

8 M. I. D. Mardjan, A. Mayooufi, J.-L. Parrain, J. Thibonnet and L. Commeiras, *Org. Process Res. Dev.*, 2020, **24**, 606–614.

9 TURBOMOLE V7.5 2020, a development of University of Karlsruhe and Forschungszentrum Karlsruhe GmbH, 1989–2007, TURBOMOLE GmbH, since 2007; available from **https://www.turbomole.com**.

10 (*a*) P. A. M. Dirac, *Proc. R. Soc. London, Ser. A*, 1929, **123**, 714–733; (*b*) J. C. Slater, *Phys. Rev.*, 1951, **81**, 385–390; (*c*) J. P. Perdew and Y. Wang, *Phys. Rev. B: Condens. Matter Mater. Phys.*, 1992, **45**, 13244–13249; (*d*) J. Tao, J. P. Perdew, V. N. Staroverov and G. E. Scuseria, *Phys. Rev. Lett.*, 2003, **91**, 146401; (*e*) S. Grimme, J. Antony, S. Ehrlich and H. Krieg, *J. Chem. Phys.*, 2010, **132**, 154104; (*f*) F. Furche and J. P. Perdew, *J. Chem. Phys.*, 2006, **124**, 044103.

11 (*a*) F. Weigend and R. Ahlrichs, *Phys. Chem. Chem. Phys.*, 2005, **7**, 3297–3305; (*b*) K. Eichkorn, F. Weigend, O. Treutler and R. Ahlrichs, *Theor. Chem. Acc.*, 1997, **97**, 119–124.

12 A. Klamt and G. Schüürmann, *J. Chem. Soc., Perkin Trans. 2*, 1992, 799–805.

13 (*a*) S. H. Vosko, L. Wilk and M. Nusair, *Can. J. Phys.*, 1980, **58**, 1200–1211; (*b*) A. D. Becke, *Phys. Rev. A*, 1988, **38**, 3098–3100; (*c*) J. P. Perdew, *Phys. Rev. B: Condens. Matter Mater. Phys.*, 1986, **33**, 8822–8824. Erratum: J. P. Perdew, *Phys. Rev. B: Condens. Matter Mater. Phys.*, 1986, **34**, 7406.

14 (*a*) J. P. Perdew and Y. Wang, *Phys. Rev. B: Condens. Matter Mater. Phys.*, 1992, **45**, 13244–13249; (*b*) J. P. Perdew, K. Burke and M. Ernzerhof, *Phys. Rev. Lett.*, 1996, **77**, 3865–3868; (*c*) J. P. Perdew, M. Ernzerhof and K. Burke, *J. Chem. Phys.*, 1996, **105**, 9982–9985.